CHEMISTRY OF MATERIALS
Communication

Chem. Mater. **2009,** *21,* 4087–4089 4087
DOI:10.1021/cm9002433

Facile Method for the Fabrication of Vertically Aligned ITO Nanopillars with Excellent Properties

Agus Purwanto,[†] Hendri Widiyandari,[‡] Darmawan Hidayat,[§] Ferry Iskandar,[§] and Kikuo Okuyama*[,§]

[†]*Department of Chemical Engineering, Faculty of Engineering, Sebelas Maret University, Jl. Ir. Sutami 36 A, Surakarta, Central Java, 57126 Indonesia,* [‡]*Department of Physics, Faculty of Mathematic and Natural Science, Diponegoro University, Jl. Prof. H. Soedarto SH, Semarang, Central Java, 50275 Indonesia, and* [§]*Department of Chemical Engineering, Graduate School of Engineering, Hiroshima University, 1-4-1 Kagamiyama, Higashi Hiroshima 739-8527, Japan*

Received January 27, 2009
Revised Manuscript Received June 10, 2009

Tin-doped indium oxide (ITO) has been used extensively in the fabrication of displays, solar cells, sensors, and LEDs (light emitting diodes).[1−5] Deposited under optimal conditions, the specific resistivity of ITO film reaches 1×10^{-4} Ω cm with an optical transparency of more than 80%—ideal properties for transparent conducting oxide (TCO) material.[6,7] In addition, in spite of planar films, one-dimensional (1D) ITO films show promise for the performance enhancement of electronic and optoelectronic devices.[8,9] For example, ITO nanowires improve the sensitivity of ethanol detection to as high as 40 for 200 ppm ethanol with a short response and recovery time (shorter than 2 s).[3] In addition, the tailored refractive index of oblique ITO nanorods can be used as an antireflection layer to enhance the light extraction in blue LEDs.[5]

Atmospheric pressure deposition (APD) processes, such as spin coating,[10−12] dip-coating[13,14] and inkjet printing,[6,15] are good candidates for low-cost deposition. To conduct low-temperature compaction, monodispersed ITO nanoparticles (< 50 nm) with high crystallinity and conductivity are required.[1,6,16,17] Unfortunately, deposited ITO films suffer from low mechanical strength and are limited to only planar structures.[10,18] The addition of organosilane to an ITO paste reportedly improved the adhesion strength of spin-coated ITO films, but at the cost of lowered conductivity.[18]

Film fabrication using a flame reactor equipped with a deposition apparatus is one class of APD process that is new and promising. For simplicity, this method will be reffered to here as direct deposition using flame (DDF). In this process, two required steps for film production are performed simultaneously—i.e., nanoparticle fabrication and deposition. A detailed schematic diagram of the process can be found in the Supporting Information, Figure S1. Reportedly, TiO_2, Pt/SnO_2, and SiO_2-doped SnO_2 films can be successfully deposited using this method.[19−22] Control of morphology (from dense to nanopillar), which was evident in the preparation of TiO_2 films, has a direct correlation with the performance of dye-sensitized solar cells and photo watersplitting devices.

In this communication, we report an extension of the DDF method for an ITO system. Aligned ITO nanopillars (1D nanostructure) films were grown and their properties were systematically investigated. To the best of our knowledge, our proposed method is the first to report the fabrication of 1D nanostructured ITO thin film under atmospheric pressure conditions. Unlike the VLS (vapor−liquid−solid) method,[4,23−25] our method did not use a catalyst to grow the 1D structure, which ensures the purity of the product.

*To whom correspondence should be addressed. E-mail: Okuyama@hiroshima-u.ac.jp. Tel: +81-82-424-7716. Fax: +81-82-424-5494.

(1) Choi, S. I.; Nam, K. M.; Park, B. K.; Seo, W. S.; Park, J. T. *Chem. Mater.* **2008**, *20*, 2609.
(2) Elam, J. W.; Baker, D. A.; Martinson, A. B. F.; Pellin, M. J.; Hupp, J. T. *J. Phys. Chem. C* **2008**, *112*, 1938.
(3) Vaishnav, V. S.; Patel, P. D.; Patel, N. G. *Thin Solid Films* **2005**, *490*, 94.
(4) Xue, X. Y.; Chen, Y. J.; Liu, Y. G.; Shi, S. L.; Wang, Y. G.; Wang, T. H. *Appl. Phys. Lett.* **2006**, *88*, 201907.
(5) Kim, J. K.; Chhajed, S.; Schubert, M. F.; Schubert, E. F.; Fischer, A. J.; Crawford, M. H.; Cho, J.; Kim, H.; Sone, C. *Adv. Mater.* **2008**, *20*, 801.
(6) Buhler, G.; Tholmann, D.; Feldmann, C. *Adv. Mater.* **2007**, *19*, 2224.
(7) Viespe, C.; Nicolae, L.; Sima, C.; Grigorlu, C.; Medianu, R. *Thin Solid Films* **2007**, *515*, 8771.
(8) Cui, Y.; Wei, Q. Q.; Park, H. K.; Lieber, C. M. *Science* **2001**, *293*, 1289.
(9) Law, M.; Greene, L. E.; Johnson, J. C.; Saykally, R.; Yang, P. D. *Nat. Mater.* **2005**, *4*, 455.
(10) Al-Dahoudi, N.; Aegerter, M. A. *Thin Solid Films* **2006**, *502*, 193.
(11) Epifani, M.; Diaz, R.; Arbiol, J.; Siciliano, P.; Morante, J. R. *Chem. Mater.* **2006**, *18*, 840.
(12) Kim, S. S.; Choi, S. Y.; Park, C. G.; Jin, H. W. *Thin Solid Films* **1999**, *347*, 155.
(13) Prodi-Schwab, A.; Luthge, T.; Jahn, R.; Herbig, B.; Lobmann, P. *J. Sol-Gel Sci. Technol.* **2008**, *47*, 68.
(14) Ogi, T.; Iskandar, F.; Itoh, Y.; Okuyama, K. *J. Nanopart. Res.* **2006**, *8*, 343.
(15) Hong, S. J.; Kim, Y. H.; Han, J. I. *IEEE Trans. Nanotechnol.* **2008**, *7*, 172.
(16) Ba, J. H.; Fattakhova-Rohlfing, D.; Feldhoff, A.; Brezesinski, T.; Djerdj, I.; Wark, M.; Niederberger, M. *Chem. Mater.* **2006**, *18*, 2848.
(17) Gilstrap, R. A., Jr.; Capozzi, C. J.; Carson, C. G.; Gerhardt, R. A.; Summers, C. *J. Adv. Mater.* **2008**, *20*, 1.
(18) Al-Dahoudi, N. Ph.D. Dissertation. Universität des Saarlandes, Saarbrücken, Germany, **2003**.
(19) Thimsen, E.; Rastgar, N.; Biswas, P. *J. Phys. Chem. C* **2008**, *112*, 4134.
(20) Thimsen, E.; Biswas, P. AlChE J. **2007**, *53*, 1727.
(21) Madler, L.; Roessler, A.; Pratsinis, S. E.; Sahm, T.; Gurlo, A.; Barsan, N.; Weimar, U. *Sens. Actuators, B* **2006**, *114*, 283.
(22) Tricoli, A.; Graf, M.; Pratsinis, S. E. *Adv. Funct. Mater.* **2008**, *18*, 1969.
(23) Vomiero, A.; Ferroni, M.; Comini, E.; Faglia, G.; Sberveglieri, G. Nano Lett. **2007**, *7*, 3553.
(24) Wan, Q.; Wei, M.; Zhi, D.; MacManus-Driscoll, J. L.; Blamire, M. G. Adv. Mater. **2006**, *18*, 234.
(25) Wan, Q.; Dattoli, E. N.; Fung, W. Y.; Guo, W.; Chen, Y. B.; Pan, X. Q.; Lu, W. Nano Lett. **2006**, *6*, 2909.

Published on Web 08/17/2009

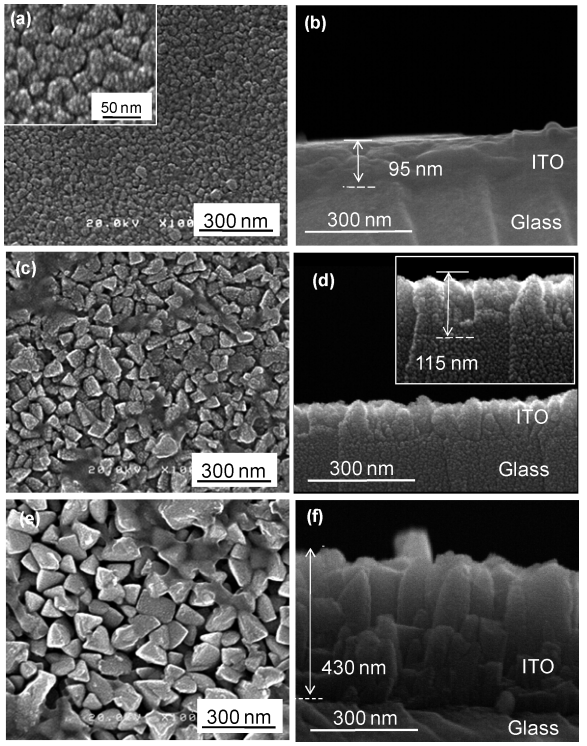

Figure 1. Field emission scanning electron microscopy (FE-SEM) image of ITO films prepared at different deposition times: (a, b) 10, (c, d) 30, and, (e, f) 60 min. The variation in deposition times can be used to control the film morphology.

The morphology and cross-section of the as-grown ITO film as a function of deposition time is shown in Figure 1. An FE-SEM image of the top view of the ITO film deposited for 10 min is shown in Figure 1a. The experimental condition for deposition used a CH_4 flow rate of 1.5 L/min and a precursor rate of approximately about 4 mL/h. The as-grown film was composed of almost spherically monodispersed grains with sizes that ranged from 27 to 35 nm (mean grain diameter is 32 nm) and with good uniformity. For comparison, the particle size was collected in a bag filter, which was equipped after the deposition apparatus was determined. According to the SEM image, particle sizes ranged from 30 to 50 nm (see the Supporting Information, Figure S3). The size of the collected ITO particles was larger compared to the size deposited in the film due to the crystal growth along the flame reactor. The observation of the cross-sectional image (Figure 1b) indicated that ITO film was planar and dense with a thickness of approximately 95 nm. With a further increase in deposition time, ITO films with different nanostructures can be obtained. For a deposition time of 30 and 60 min, the ITO films are composed of a discrete morphology of mostly triangle-shaped particles (Figure 1c,e). Cross-sectional images of ITO films grown for 30 min show a pyramidlike structure with a height of approximately 115 nm (Figure 1d). Finally, a pillar-like structure of ITO film with a height of approximately 430 nm and pillar diameters ranging from 60 to 90 nm was observed in the film deposited for 60 min.

The XRD pattern of ITO films deposited at various deposition times is shown in Figure 2. This shows that the

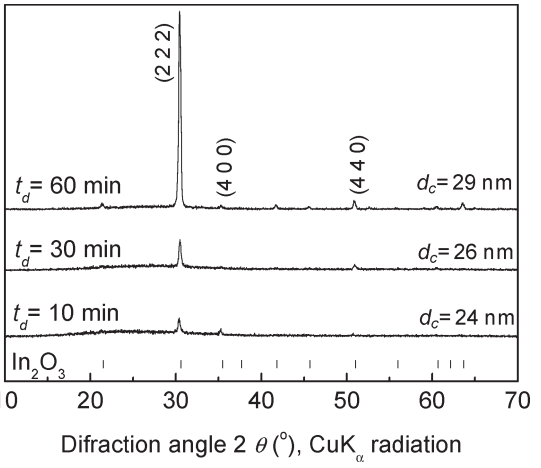

Figure 2. X-ray diffraction (XRD) spectra of ITO films deposited at different deposition times. The XRD spectra fits well with the JCPDS no 06−0616 cubic bixbyite structure of In_2O_3.

XRD spectra of as-grown ITO films fit well with JCPDS no 06−0616 (space group: *Ia*3, a = 10.118 Å), which indicates the cubic bixbyite structure of In_2O_3.[16,17] All films were prepared using a Sn^{4+} concentration of 4.5 mol % with a total precursor concentration of 0.02 M. The lattice spacing values of ITO films deposited for 10 min at (222), (400), and (440) orientations are 2.82, 2.45, and 1.76 Å, respectively. For the same lattice orientations, the lattice spacing values of the JCPDS reference are 2.92, 2.52, and 1.79 Å, respectively. The lattice spacing of flame-deposited ITO films was found to be smaller compared with that of the references. It is known that the doping of Sn^{4+} ions into In_2O_3 would occupy the In^{3+} ion positions in the crystal structure. The atomic radius of Sn^{4+} and In^{3+} is 1.72 and 2.0 Å, respectively. Because Sn^{4+} has a shorter atomic radius than In^{3+}, the replacement of In^{3+} ions by Sn^{4+} ions would reduce the lattice spacing, as shown above. The reduction of lattice spacing was consistent with the differences in the Sn concentrations (see the Supporting Information, Figure S4). In addition, the crystallite sizes determined using Scherer's equation from the line broadening of the (222) reflection were 24, 26, and 29 nm for ITO films deposited for 10, 30, and 60 min, respectively. The XRD spectra showed no discernible SnO or SnO_2 peaks, which was an indication of the phase purity of the as-grown films.[17] Moreover, from SEM with EDS analysis, the ITO films comprised of 95.3 at % In and 4.7 at % Sn indicated the preservation of components during film formation.

The transmittance of the ITO films as a function of deposition time is shown in Figure 3. In the case of ITO film deposited for 10 min, a typical transmittance of ITO films was observed in which the transmittance decreased as the wavelength decreased, which is similar to the ITO film grown using other methods.[7,10] In general, transmittance was more than 80% for the observation wavelength from 400 to 800 nm. Pyramid-like ITO films (deposited for 30 min) exhibited a very high transmittance of 92.82% for a wavelength of 441 nm with a bluish film color. A high transmittance at more than 90% was observed

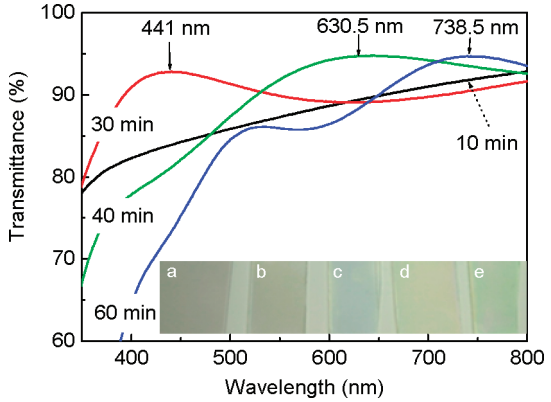

Figure 3. Transmittance spectra of ITO films deposited at different deposition times. Inset: photograph images of ITO films. (a) Commercial, (b) 10 min, (c) 30 min, (d) 40 min, and, (e) 60 min. The transmittance property of ITO film can be tuned using a variation of deposition time.

when the wavelength ranged from 394 to 541 nm. The ITO films deposited for 40 min exhibited a transmission of 94.74% at a wavelength 630.5 nm (transmittance of more than 90% was observed for a wavelength higher than 527 nm). In addition, ITO nanopillar film (deposition time 60 min) showed high transmittance (peaked at 94.73%) in the wavelength range of 738.5 nm and was yellowish in color. In a wavelength at higher than 650 nm, ITO films exhibited a light transmittance of more than 90%. The high transmittance in a wide wavelength in visible light is a potential future optoelectronic application. For example, such ITO films could enhance the efficiency of a polymer/dye-type solar cell in which a wavelength of high transmittance could be matched with the maximum absorption wavelength of semiconductors/dye to give the maximum photon absorption.

The electrical conductivity of ITO thin films was evaluated using a 4-probe method. To find the optimal concentration of Sn^{4+} for electrical conductivity, the Sn doping concentration was varied in the preparation of planar structures (deposited for 10 min) (see the Supporting Information, Figure S5a). ITO films were found to have good conductivity with a specific resistance of $(4.83 \pm 0.19) \times 10^{-3}$ Ω cm at an optimal doping concentration of Sn (4.5 mol %). At lower and higher doping concentrations, the specific resistivity increased. From the literature, it was found that the variation in sheet resistivity for ITO films as an effect of Sn concentration originates from the fluctuation of electron density in the crystal.[18] Substitution of the In^{3+} ion with the Sn^{4+} ion releases one electron in the crystal lattice, which contributes to the conductivity of the ITO films. In the case of a high Sn concentration, the films may form defects, such as SnO, Sn_2O. and Sn_2O_4, which act as electron traps and imply reduced conductivity.

In addition, the reduction of ITO films in the elevated temperature of forming gas (5% H_2/95% N_2, 300 mL min^{-1}) conditions can be used to reduce specific resistivity. The reduction proceeded for 1 h at a heating rate of 10 °C min^{-1}. An increasing reduction temperature was found to reduce the specific resistivity of ITO films with the optimal reduction temperature being in the range of 450 to 550 °C (see the Supporting Information, Figure S5b). During the reduction process, oxygen ions in the ITO crystals were reduced creating oxygen vacancies that remarkably increased the carrier concentration. As a result, the conductivity of ITO films was improved significantly. ITO film reduced at 550 °C exhibited specific resistivity, $(6.26 \pm 0.33) \times 10^{-4}$ Ωcm, that was close to a standard gas-phase deposition method (in the range of 1×10^{-4} Ω cm).[6] In addition, after reduction to 450 °C for 1 h, the sheet resistances of ITO nanopillar films were 257.7 ± 8.9 and 122.5 ± 8.1 Ω□ for the deposition times of 30 and 60 min, respectively. This value is higher compared with that of the planar film because of the presence of a void in the interspacing of the pillar structure. Practically, the conductivity of nanopillar ITO films can be improved by increasing the reduction temperature as well as the reduction time. In addition, a strong film adhesion was observed in which films did not peel off after the tape test.

In conclusion, we reported a facile deposition technique (DDF method) used to prepare high-performance, vertically aligned ITO nanopillars with excellent properties. The characterization of optical properties indicates that the ITO films have high transparency in the visible light range. In addition, the ITO films have a low specific resistivity on the order of 1×10^{-4} Ω cm. Such ITO films may open new avenues for the improvement of optoelectronic device performance by increasing the contact area of active material semiconductors with electrodes. Furthermore, this deposition technique offers a low-cost process for ITO film deposition that could potentially reduce the price of TCO.

Acknowledgment. We thank Dr. Eishi Tanabe from Hiroshima Prefectural Institute of Industrial Science and Technology for helping with SEM-EDS analysis, and for his discussions.

Supporting Information Available: The synthesis procedure, a schematic diagram of the experimental setup, and characterization data of ITO thin films (PDF). This material is available free of charge via the Internet at http://pubs.acs.org.